Chemical Engineering Science 131 (2015) 63–75

Contents lists available at ScienceDirect

Chemical Engineering Science

journal homepage: www.elsevier.com/locate/ces

A comparative study on optical techniques for the estimation of granular flow velocities

Thomas Hagemeier [a,*], Matthias Börner [a,b], Andreas Bück [a], Evangelos Tsotsas [a]

[a] NaWiTec, Thermal Process Engineering, Otto-von-Guericke University Magdeburg, Universitaetsplatz 2, 39106 Magdeburg, Germany
[b] Hüttlin GmbH, a Bosch Packaging Company, Hohe-Flum-Str. 42, 79650 Schopfheim, Germany

HIGHLIGHTS

- Four measurement techniques (FOP, LDV, PIV, PTV) for two-phase flow in fluidized bed.
- High-speed imaging for individual particle identification and tracking.
- Comparison of techniques capabilities, limitations and development potentials.
- Recommendations and guidelines for applications with industrial or research focus.

GRAPHICAL ABSTRACT

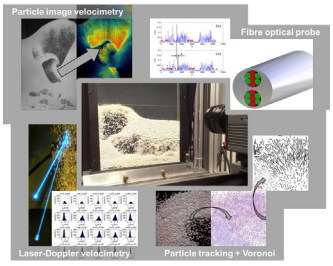

ARTICLE INFO

Article history:
Received 11 December 2014
Received in revised form
19 March 2015
Accepted 27 March 2015
Available online 3 April 2015

keyword:
Granular flow
2D fluidized bed
fiber optical probe
laser Doppler velocimetry
particle image velocimetry
particle tracking velocimetry

ABSTRACT

The evaluation of particle velocities in fluidized beds has improved the understanding of ongoing micro- and macro-processes significantly. Several measurement techniques are available in order to estimate single particle velocities as well as granular flow velocities in terms of velocity fields. All of those techniques feature individual advantages and shortcomings, which have been reviewed at various occasions, in particular by Werther (1999) and Horio et al. (2003) or recently by Sutkar et al. (2013). Often, the reviewers presented facility specific findings, which are not to be generalized.

Therefore, our study focuses on the comparison of four different measurement techniques, namely fiber optical probe (FOP), laser Doppler velocimetry (LDV), particle image velocimetry (PIV) and particle tracking velocimetry (PTV), which have been applied under identical conditions at one and the same flat fluidized bed facility. Consequently, results obtained with the different techniques feature identical system characteristics and can be compared to derive general conclusions.

1. Motivation and fundamentals

Knowledge about particle or particle cluster velocities in granular or multiphase systems is essential to characterize the flow conditions and dynamics. Spatially resolved particle velocities identify the solids flow field and further enable conclusions about the fluid flow, if e.g. particles have the size of traces. A complex example of a multiphase flow is a gas–solid fluidized bed. The particle velocity information is here of particular interest to describe the circulatory motions of the solids. Recently, particle velocities have been measured to investigate particle re-circulation times (Cronin et al., 2010; Depypere et al., 2009), dead zones (Börner et al., 2013) or solids exchange rates between two or more considered compartments (Börner et al., 2014; Hussain et al., 2014). Particle velocity measurements are also performed to calibrate DEM-CFD simulations (Hoomans et al., 2001). Therefore, a precise quantification of particle velocities within the process chamber is of enormous value to modern system analysis and macroscopic modeling approaches.

The objective of this study is to present a broad overview of optical measurement techniques for the acquisition of particle

* Corresponding author. Tel.: +49 391 6712322.
E-mail address: Thomas.Hagemeier@ovgu.de (T. Hagemeier).

http://dx.doi.org/10.1016/j.ces.2015.03.045
0009-2509/

dynamic properties, ranging from averaged solid phase velocity and solid volume fraction to individual particle trajectories or particle–particle collisions. Moreover, experiments with four different measurement techniques on one and the same fluidized bed apparatus yield truly comparable information. Without variations caused by differences in apparatus design or operating conditions, it is the first time that four measurement devices have been applied to one fluidized bed. A comparison of the results obtained with the different measurement techniques reveals accuracy and eventually limitations of the different devices.

Generally, there are many ways to gather information concerning particle dynamics in fluidized beds, as described for instance by Bhusarapu et al. (2006). However, commonly used optical measurement techniques are not applicable to dense particulate flow as found in full scale fluidized beds. Alternative tomographic techniques are available for small scale equipment. These methods like PEPT (Positron Emission Particle Tracking) (Hoomans et al., 2001; Depypere et al., 2009) or magnetic monitoring (Mohs et al., 2009) are typically very expensive and limited to small scale fluidized beds with tracer particle. 3-dimensional trajectories of tracers can be obtained, but no instantaneous flow fields. In order to expose and concentrate on the applicability of optical measurement techniques a generic flat fluidized bed was utilized in our investigations, as is described in detail in Section 2. Though this design provides an almost 2D flow pattern, the optical measurement techniques have to be adapted before use on it. Such a flat fluidized bed has been critically discussed by Börner et al. (2014). Particle–wall friction has been determined as major influencing factor. A general applicability in comparison to true 3D fluidized beds was proven. The fiber optical probe (FOP), laser-Doppler velocimetry (LDV), particle image velocimetry (PIV) and particle tracking velocimetry (PTV) have been applied to this unique apparatus to obtain data for particle dynamics which are then compared with each other. The experimental procedure and the comparison of results reveal advantages and disadvantages of each technique. Handling, performance and data quality can be evaluated independently of facility specific parameters, which are usually unknown when reviewing existing literature. A general overview of research concerning the estimation of particle motion in flat fluidized bed systems using optical measurement techniques is provided in Table 1.

Eventually, we are able to yield recommendations when and how to use a technique in the situation of dense particulate flow.

The paper is organized in the following way. Section 3 is used to describe the measurement techniques individually. Each description relies on an extensive literature survey, in particular regarding the application to fluidized beds and the estimation of particle dynamics. Section 2 describes the experimental setup used in this work and gives information concerning the particle system and operating conditions. All experimental results and comparisons are presented in Section 4. Finally, Section 5 contains recommendations and describes the advantages and disadvantages of the different measurement techniques. This can be a guide for an appropriate selection of measurement techniques and settings for the complex flow conditions in fluidized beds.

2. Experimental configuration

For the ease of understanding, the experimental facility shall be introduced briefly, before giving detailed descriptions of the individual measurement techniques.

All investigations have been conducted at a pseudo-2D fluidized bed. A corresponding sketch of the experimental facility is shown in Fig. 1. The dimensions of the fluidized bed are $300 \times 20 \times 1000\ \mathrm{mm}^3$ in width, depth and height. In order to provide optical access for various measurement devices, front and back are made of shatterproof glass. Additional surface treatment (plastic film) prevents the material from abrasion due to intense particle contact. The side walls are made of aluminum.

For monitoring purposes, several thermocouples and pressure sensors are connected to the fluidized bed. The air flow is generated by in-house compressed air supply and fixed to a certain flow rate via mass flow controller. For homogenous gas inlet at the bottom of the fluidized bed, a sintered metal plate was used with a thickness of 3 mm and a mean pore size of 100 μm.

The particle system within the rectangular vessel consisted of spherical γ-Al_2O_3 particles with a diameter of $d_p = 1.8$ mm and a density of $\rho = 945\ \mathrm{kg/m}^3$. A bed mass of $m_{bed} = 0.515$ kg fixed the initial height of the static bed to $h_{pb} = 150$ mm. All experiments have been conducted at a fluidization velocity of 3 times the minimum fluidization velocity $u_{mf} = 0.56$ m/s.

The velocity measurements using the FOP were conducted with a special back-wall, which provided a certain number of openings where the probe penetrated the particle bed. In order to keep the intrusion effect as low as possible, the probe head ended at the same level as the inner wall surface. Therefore, the particle flow remained undisturbed, except for the different material in the wall. The LDV measurements have been carried out at exactly the same locations, to ensure directly comparable results for the two pointwise measurements.

During the PIV measurements, the process chamber was captured up to a height of $y = 500$ mm on each double frame image (shown as blue box in Fig. 1). This corresponded to a spatial resolution of $sf = 1.96$ pixel/mm. Consequently, only global intensity patterns were imaged without resolving individual particles.

In contrast, PTV measurements required a higher spatial resolution. The four fields of view, indicated as red boxes in Fig. 1, ranged from $y = 130$ mm to $y = 215$ mm above the bottom of the process chamber. Each field of view resolved an area of $85 \times 85\ \mathrm{mm}^2$ and slightly overlapped with the neighbor region. Also in contrast to the PIV technique, two halogen lamps have been used here, each with 400 W electrical power.

3. Measurement techniques

3.1. Fiber optical probe (FOP)

Fiber optical probes have been designed in the 1970s and 1980s of the last century, in order to investigate solids motion in dense multiphase flows (Savage, 1979; Ishida et al., 1980; Patrose and Caram, 1982). The technique is based on the measurement of light reflections of solid particles, and has been primarily applied to measure bubble and particle velocities in highly unsteady and heterogeneous particulate systems. Here, the fiber optical probe shows advantages as a fast and robust measurement technique with high signal-to-noise ratio (SNR). Besides the velocity information, the solid volume fraction can be measured as well (Hartge et al., 1988). The use of fiber optical probes is limited to local measurements inside a multiphase system and intrusive (Louge, 1997). Several applications have been presented for circulating fluidized beds (Herbert et al., 1994; Werther, 1999; Johnsson and Johnsson, 2001; Xu and Zhu, 2010), bubbling fluidized beds (Dencs, 1995; Zhang et al., 1998) or spouted beds (José et al., 2006; Wang et al., 2009). Further applications of a fiber optical probe have been presented for chute flows (Ahn et al., 1991; Hsiau and Hunt, 1993), verifying a measurement error of 2–3% for the mean particle velocity, and for rotating drums (Boateng and Barr, 1997).

In the last decades several fiber arrangements in the probe tip (Tayebi et al., 1999; Zhu et al., 2001) or alternative light sources (Hartge

Table 1
Literature survey on experimental investigations of particle dynamics in rectangular fluidized beds, including information concerning the measurement technique, aspect ratio of apparatus depth to particle diameter and objective of the respective study.

Author	Measurement technique	Aspect ratio	Research focus
Hagemeier et al. (in press)	PTV	11.1	Development of discrete particle tracking for dense particulate flow
Cloete et al. (2013)	PIV	25–214.3	Comparison of PIV and 2D two-fluid model (TFM) simulations for estimating the applicability of 2D simulation approaches
de Jong (2013)	PIV, digital image analysis (DIA)	25–37.5	Particle fluidization and gas flow in fluidized beds with horizontal membrane tubes
Sánchez-Delgado et al. (2013)	PIV, DIA	6.25–8.33	Estimation of particle circulation time in fluidized bed
Sutkar et al. (2013)	PIV	20	Combined experimental and numerical study of particle fluidization and introduction of a flow regime map
Agarwal et al. (2012)	PIV, DIA	16.9–23.1	Effect of multiple jets on fluidization of Geldart class B and D particles
de Jong and Odu (2012)	PIV, DIA	6–30	Improvement of DIA processing using discrete phase modeling
Mychkovsky et al. (2012)	LDV	15.15	Estimation of gas and particle velocities in jets using different tracer particles
Xu and Zhu (2012)	FOP	66.2–83.6	Development of a new image based method for estimation of cluster velocities in circulating fluidized bed
Börner et al. (2011)	PIV, DIA	11.1	Investigation of particle residence times in various fluidized bed configurations
Hernández-Jiménez et al. (2011)	PIV, DIA	8.33–12.5	Investigation of bubble coalescence using DIA-PIV and computational fluid dynamics (CFD)
Buijtenen et al. (2011a)	PIV, DIA	6.5–10	Effect of restitution coefficient on particle dynamics in spouted fluidized beds
Buijtenen (2011)	PIV, DIA	6.7	Estimation of the effect of multiple-spouts on particle fluidization
Sánchez-Delgado et al. (2010)	PIV, DIA	6.25–8.33	Characterization of the influence of bubbles on the particle velocity and velocity fluctuations
Wang et al. (2009)	FOP	218–906	Estimation of velocity profiles of size distributed solids in the feed region of a circulating fluidized bed
Laverman and Roghair (2008)	PIV, DIA	25–37.5	Combined PIV-DIA investigation of bubbling fluidized beds
Liu et al. (2008)	PIV	7.5	Investigation of solid phase velocity field including spectral analysis and granular temperature in spouted beds
Zhao et al. (2008)	PIV	7.5	Investigation of particles dynamics in spouted bed with internal riser using PIV measurements and discrete element method (DEM) simulations
Laverman et al. (2007)	PIV, DIA	25–37.5	Investigation of particle circulation and bubble behavior
Santana et al. (2005)	PIV	16.7	Description of bubble eruption mechanism
Link et al. (2004)	PIV, DIA	6	Combined estimation of particle velocity and solid volume fraction using PIV and DIA in spouted beds
Ibsen et al. (2002)	LDV	1900–3064	Measurement of particle velocity profiles and velocity fluctuations in a pilot scale circulating fluidized bed
Zhou et al. (2000)	LDV	444	Investigation of turbulence structures using wavelet transform of LDV signals for solid phase velocity
Zhou et al. (1995)	FOP	685	Measurement of particle velocity profiles in a circulating fluidized bed
Lim and Agarwal (1992)	Shadow imaging, FOP	30–50	Derivation of correlations for bubble size/shape and velocity for single bubbles and bubble swarms

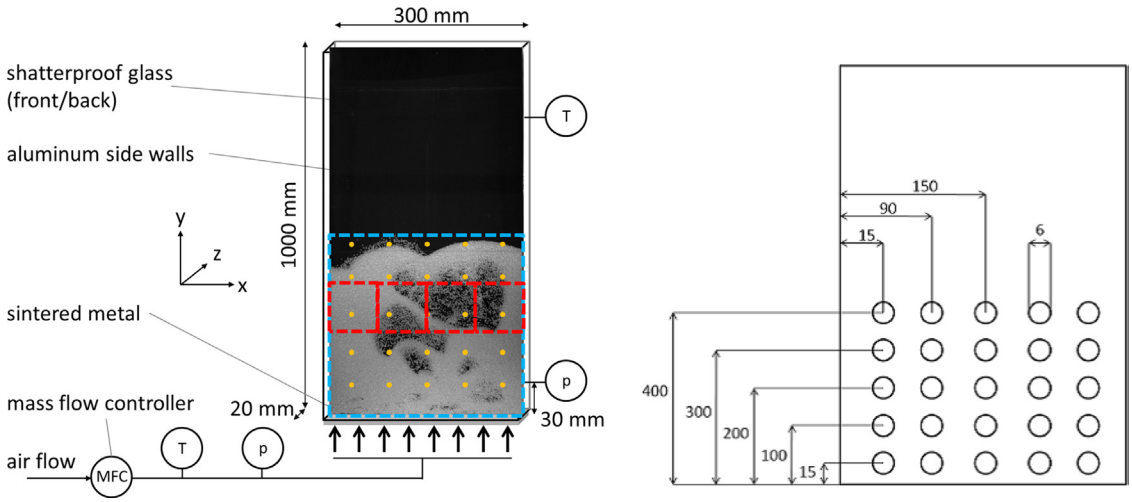

Fig. 1. Sketch of pseudo-2D fluidized bed facility (top), with exemplary fluidization pattern; yellow dots represent measurement points for FOP and LDV, the PIV field of view is bounded in light blue, the PTV fields of view are bounded in red. The grid for FOP and LDV measurements is shown at the bottom. (For interpretation of the references to color in this figure caption, the reader is referred to the web version of this paper.)

et al., 1988) have been reported, to improve the measurement accuracy. Generally, the measurement uncertainty is reasonably low after performing an appropriate calibration of the system, as shown e.g. by Li et al. (2009). However, there are some shortcomings of the light reflection method, mainly relying on the competition of light transmission and light reflection, which depend on the solid volume

fraction, as shown by Louge (1997). The transmitted light intensity is reduced with increasing distance to the probe, while an effect of the distance on the reflected light could not be observed. Nevertheless, the reflected light intensity strongly depends on the particle size and it might be affected by the occurrence of blind spots (Rensner, 1991; Beaud and Louge, 1996). These blind spots can be e.g. passing gas bubbles in a heterogeneous fluidized beds. Cocco et al. (1995) showed that issues of blind spots can be reduced when using fiber pairs. Rensner and Werther (1993) described the spread of light beams by a mathematical model. They proved that the measuring volume is strongly depending on the solid volume fraction in front of the probe tip.

The fiber optical probe used in our investigations consists of a light source which are light emitting diodes (LED's) having an infra-red spectrum in the range of 800–1400 nm. The light is transmitted from the light source to the probe tip by three emitting fibers to illuminate the measurement volume in front of the probe tip. The emitted light intensity decreases exponentially with distance to the probe tip. So, the maximum measurement depth is limited to 4 mm. The reflected light by solids reaching the probe tip is transmitted back by four receiving fibers onto a photo diode. The received light intensity is transformed into a voltage signal between 0 and 12 V. A schematic sketch of the probe is shown in Fig. 2. The probe offers two detection positions, each with two opposing receiving fiber pairs and three emitting fibers in-between. The distance between the two receiving fiber pairs at one detection position is 180 µm, while the distance between the identical pairs at the different detection positions is 2250 µm. This arrangement allows the detection of either small or large particles.

The determination of particle velocity is based on the analysis of two voltage signals of both independent receiving fiber pairs. Solids passing the measurement volume will cause a voltage signal first in one receiving fiber pair and after a while in the other receiving fiber pair. The time shift between both recorded signals can be obtained by a cross-correlation algorithm. Since the distance between both receiving fibers is known, the particle velocity can be obtained. It should be strictly emphasized that an intensive preparation and adjustment of the probe is essential to obtain accurate and reliable results. Attention has to be paid to the fiber arrangement, measuring facility and the flow direction of solids. Unrealistic results and misinterpretation are often the consequence of a wrong application of the probe, like in San José et al. (1998), Olazar (1998) or Link et al. (2009). Regarding the paper presented by San José et al. (1998) and Wu and Berrouk (2009) showed the inaccuracy of results by employing a simple force balance. With the here applied fiber optical probe and fiber arrangement, particle velocity can be measured directly and accurately only for particles crossing vertically to the fiber arrangement (particles moving from up to down or vice versa). If particles pass is oblique or parallel to the fiber pair arrangement, the particle crossing path is not equal to the direct distance between the fiber pairs. If this constant distance is still used, erroneous results will be the consequence. For instance, a particle path parallel to the fiber arrangement ends up in a particle velocity of infinity, since the passing particle is detected in both fibers at the same time. In this regard, if a two-dimensional particle flow exists, the particle velocity vector can be obtained by a x, y-velocity component measurement and flow angle reconstruction. The flow angle of particles path can be obtained from the apparent x, y-velocity components

$$\alpha = \arctan \frac{v_x^*}{v_y^*}. \tag{1}$$

v_x^* and v_y^* are the apparently measured velocity components and α is the flow angle of the particle path. The v_x^* velocity component is measured with horizontal fiber arrangement and v_y^* with vertical fiber arrangement, respectively. If the flow angle is known, the true

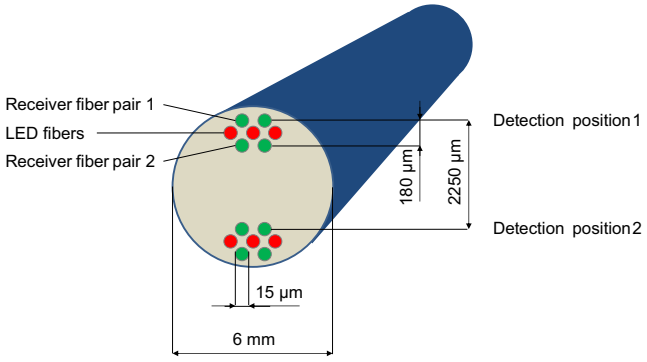

Fig. 2. Emitting and receiver fiber arrangement of the optical probe.

velocity components can be determined

$$v_x = \frac{s}{t \cos \alpha} \tag{2}$$

$$v_y = \frac{s}{t \sin \alpha}. \tag{3}$$

Here, s is the distance between the receiving fibers and t the time determined by the cross-correlation. In a three-dimensional particle flow, where particles additionally move towards and away from the probe, the velocity vector cannot be determined unambiguously by this type of fiber optical probe.

Further on, it is recommended to filter the voltage signal for blind spots/gas bubbles before applying the cross-correlation. From unfiltered signals usually some averaged value of bubble rise velocity and particle velocity is determined. To achieve signal components only related to the particle velocity, a segmentation of the entire measurement signal into N-segments with a discrete number of measurement values is proposed. If a certain number of measurement values inside one segment is below a threshold value, the segment can be associated to a gas bubble. Segments of gas bubbles should not be used in the analysis for particle velocity. Finally, an averaged particle velocity is determined. To obtain averages with a statistical certainty, a measurement time of 180 s at a recording frequency of 30 kHz is accounted for.

3.2. Laser Doppler velocimetry (LDV)

Laser Doppler velocimetry is a non-intrusive measurement technique for the estimation of particle velocities. It is based on the principles of Mie-theory and the associated evaluation of scattered light frequencies. Light is scattered by particles passing a measuring volume (fringe pattern) which is established by two crossing laser beams. Usually, the beams are inclined by a small angle to each other, while one of the beams features a shift frequency to assign positive and negative velocities. Generally, the velocity component in plane with the two laser beams is measured.

We omit further details concerning the general methodology and accuracy of LDV since it is well known and described in research papers (Durst et al., 1976) or comprehensive textbooks (Durst et al., 1981; Albrecht et al., 2003; Tropea et al., 2007).

LDV can be applied in front or back scattering configurations, using separate or integrated receiver, respectively. Obviously, the application of this device is limited due to the optical access to the system. Occluded particles are excluded from any evaluation of particle velocity. Thus, velocity measurements can be carried out only on front-layer particles. Despite these limitations, LDV is one of the most commonly used measurement devices in experimental studies of dilute particulate multiphase flows. The application to

dense systems is still an exception, as the following literature survey shows.

Most significant contributions concerning LDV measurements in two-phase flows have been made by Tsuji and Morikawa (1982) and Tsuji et al. (1984), who described the application of LDV to investigate air–solid pipe flows of different orientations. Major part of their work was dedicated to adapt the measurement technique and signal processing. The application of LDV to obtain velocities of particles with diameters up to 4 mm is most relevant for our study. Using a front scattering approach, they showed how large particles affect the Doppler burst signal. Generally, particles of a few millimeters inhibit signals caused by front scattered light. However, using a back scattering approach, the light intensity increases and velocity estimation is possible, as shown in our results.

Afterward, only few research groups actively used LDV for experimental investigations, mainly in the area of circulating fluidized beds. Ibsen et al. (2002) discussed the aspect of sampling time and number of samples, since they are crucial for the estimation of small and large scale fluctuations in the fluidized bed. Moreover, the statistical error was evaluated to 0.8% for the measured velocity and 1% for the rms, considering 5000 samples.

Breault et al. (2005) reported the combined application of a LDV system together with a particle imaging device. They measured the velocity and derived the granular temperature for cork particles of 800 μm diameter, which appears rather large compared to the measuring volume length (l=1.5 mm). Similar to our experiments, they used LDV to acquire particle velocities in direct vicinity (1 mm distance) of the inner wall of the fluidized bed. Later on, Breault et al. (2008) derived dispersion coefficients in addition to granular temperature values. They also discussed in detail how granular temperature estimation depends on the temporal resolution of LDV measurements. LDV data are not valid for granular temperature evaluation when particle collision frequency is larger than the sampling rate of the measurement.

The statistics of granular surface flows was in focus of Kellay et al. (2007), who exposed the highly intermittent properties of the granular temperature, estimating the power spectrum and probability density functions of velocity fluctuations. Their results confirm that energy dissipation occurs in different terms for granular flows than in fluid flows. An adapted experimental approach has been introduced by Chemloul and Benrabah (2008). It is based on the principles of laser-Doppler technique, but accounts for individual velocities of solid–liquid two-phase flow. Large particles show increased pedestal amplitude compared to small particles or tiny tracers. Therefore, they were able to acquire data for slip velocity of the suspension, based on filtered signal analysis. Moreover, they derived information on how particles modify turbulence. However, the technique is limited to rather dilute systems, when measurements in three dimensions are desired. Laser beams are diffracted if the solid volume fraction exceeds 2%.

The LDV measurements in this study have been conducted using a commercial hardware system provided by Polytec, which was operated as backward-scattered-light system. Scattered light signals are received only from the first particle layer due to occlusion. Mainly, two aspects have to be regarded during system installation:

1. The measuring volume has to be placed properly inside the process chamber. It should be located close to but not inside the glass front.
2. The signal gain has to be set to a low value, in order to inhibit overload which is commonly encountered when working with large particles in backward-scattering mode.

The laser system and translation stage were controlled with an in-house Labview software. A summary of the hardware and software LDV settings used to estimate particle velocities is given in Table 2. System settings have been validated by fixing a single particle to a rotating wheel and measuring the particle velocity. A good agreement was observed for the measured particle velocity and the corresponding rotation speed. The deviation between measurement and prediction was below 10% which ensures reasonable results with our setup, even for particles larger than the measurement volume.

Table 2
Hardware and software settings used in the LDV measurements.

Device	Setting
Laser	Polytec
Wave length	λ=806 nm
Power	P=40 mW
focal length	f=310 mm
Beam spacing	d_B = 60 mm
Beam half angle	θ=5.5°
Fringe spacing	d_F = 4.2 μm
Shift frequency	f_s = 3 MHz
Gain	12 dB
Filter	10 MHz
Signal processing	
Mean velocity	0 m/s
Velocity range	6 m/s
Number of samples in fast Fourier transformation (FFT)	512
Trigger threshold	800 mV
Sampling rate	12,500 kHz

3.3. Particle image velocimetry (PIV)

Particle image velocimetry (PIV) is a non-intrusive, image-based measurement technique to obtain velocities of tracers and particles inside a flow. In the PIV procedure rapidly recorded double frame images are taken. Particle shifts between the two recorded images are determined by a cross-correlation algorithm. The PIV is based on the correlation of intensity distribution, and no direct particle tracking takes place. From the recording frequency of the camera the time gap between the two images is known, so that in addition to the particle shifts the particle velocity can be determined. To obtain a highly resolved particle flow field, the recorded images are meshed into subdomains, so-called interrogation areas. On each interrogation area the cross-correlation is applied.

The PIV principle was firstly introduced by Adrian (1991) and Keane and Adrian (1991), and has been later summarized by Westerweel (1997) and Raffel et al. (2007). Rix et al. (1996) were the first to apply the PIV for the investigation of fluidized beds. They investigated particle conveying and discharge in the free-board area. Further examples of PIV applications in fluidized beds are shown by Bokkers et al. (2004) for the investigation of mixing and segregation behavior, Lim et al. (2007) for vibrating liquid fluidized beds and Liu et al. (2008) for spouted beds with improved PIV-algorithm for large velocity gradients.

Usually in PIV theory the illuminated plane is realized by a thin laser light sheet. However, this works only for fluid flows with sparsely seeded tracer particles. In densely seeded multiphase flows, like fluidized beds, the laser cannot penetrate through the particle flow. Consequently, a head-on illumination has been used instead. In this study, eight halogen lamps have been applied to illuminate the scene, each lamp with 50 W electrical power. The lamps are supplied by a 12 V DC generator to avoid light fluctuations caused by the 50 Hz AC electricity grid. The drawback of head-on illumination is the use of larger particles. Particles need to be of at least three pixels

in diameter. In contrast to laser illumination, particles can consist of down to one single pixel.

Generally, a high contrast between particles and background is required to ensure accurate results. This applies for all imaging techniques including PTV which is described in the following section. When properly adjusted, PIV measurements show a high accuracy; Stanislas et al. (2005) give a value of 1%.

The PIV measurements in this study have been conducted using a commercial hardware system provided by LaVision together with the associated software tool DaVis 7.2. A summary of the applied PIV settings is listed in Table 3. It comprises camera settings and parameters for the PIV algorithm. The measurement time was systematically analyzed. A measurement time of 5 s was found to yield identical information as measurement times of 50 or 100 s. This ensures a direct comparability with PTV. Moreover, it proves that quasi-stationary fluidization behavior can be observed already with short observation times. Further information concerning the experimental setup is given in Section 2.

3.4. Particle tracking velocimetry (PTV)

Particle tracking velocimetry is an image based measurement technique to quantify particle velocities in a Lagrangian reference frame. It is mainly applied in the field of fluid mechanics, in particular to liquid flows. There are several PTV algorithms to estimate the particle velocity, as summarized by You et al. (2004). The major difference among these approaches is the algorithm for the search of corresponding particles in an image series.

However, there are only a few contributions describing PTV measurements in particulate multiphase flows. Capart et al. (2002) mentioned three challenges for imaging methods in the field of granular flows that make an out of the box application of PTV difficult. Namely, granular flows are (i) highly dense particulate systems, with (ii) fluctuating particle motions due to particle–particle collisions, causing discontinuous path lines and (iii) sharp velocity gradients. Consequently, the methodology of PTV cannot be used without adaptations to dense particulate flows, as for example in fluidized beds. First of all, the particle system has to be accessible for high-speed camera as well as for the illumination light, similar to the requirements for PIV. Consequently, the PTV approach is limited to pseudo-2D configurations. Moreover, the high particle density leads to correspondence problems within the tracking algorithm. In order to avoid wrong results, particles need to be identifiable, which can be achieved in two ways. One option is to seed the moving particle bed with particles with a different optical property than the majority of particles. This means tracer particles have to be colored using paint or a fluorescent dye (e.g. Natarajan et al., 1995), which is also common for PTV in gas flows (Bendicks et al., 2011). Colored tracer particles are usually added in a fraction of up to 8 % of the total particle mass (Hsiau and Jang, 1998). This yields only local particle velocity values, while the kinetic properties of the remaining particles are unknown.

The second way is to use a specific imaging method, where the particles are not only segmented, but a certain type of bed structure can be identified. In particular the Voronoï method is used to generate a net of connection lines between neighboring particles, yielding specific pattern of the particle bed. Both PTV adaptations have been applied to investigate granular flow velocities. Jesuthasan et al. (2006) provided a comprehensive review of PTV techniques together with the principles of PIV applied to granular flows. They also indicated the use of pattern matching algorithms to solve the correspondence problem in granular or densely seeded flows.

Table 3
Hardware and software settings used in the PIV measurements and post-processing.

Device	Setting
Camera	HighSpeedStar 3
CMOS sensor size	1024×1024 pixel
Gray levels	10 bit
Calibration factor	$sf = 1.96$ pixel mm
Frame rate	10 Hz
Δt of double frames	0.001 s
Illumination time	4×10^{-5} s
f-Number	4.2
Focal length	85 mm
Measurement time	5 s
PIV algorithm	
Interrogation area	16×16 pixel
Overlap	50%
Intensity offset	10 counts
Cross correlation	Standard FFT, no zero-padding
Vector processing	Median filter

3.4.1. Voronoï method

Particle tracking based on the Voronoï imaging method assumes that patterns formed by the particles within the fluidized bed are existent over a certain period of time. The Voronoï-diagram is a fragmentation of an area, here the image is taken with the high-speed camera, into a number of polygons. Each polygonal area is located around a centroid, with the restriction that all Euclidean points within a polygon are closer to its centroid than to any other centroid. The connection of one centroid with all neighboring centroids is called Voronoï star and plays a key role in the evaluation procedure. A comprehensive description of the Voronoï method for granular flows is given by Capart et al. (2002).

The method can be applied to 2 and 3 dimensions, although limitations to near-wall regions exist with dense particle packing. Stereoscopic images for 3D applications can be obtained either by using one camera which captures two perspectives in one image through a complex mirror arrangement or by two synchronized cameras (Spinewine et al., 2003). Moreover, the three-dimensional approach enables the investigation of all three velocity components as well as the estimation of volumetric solid fraction. This requires special treatment to resolve particle positions and overcome occlusion effects.

Luchnikov et al. (1999) suggested a generalization of the Voronoï–Delaunay analysis to include non-spherical particles. Despite the fact that they did not couple their approach to a particle tracking algorithm, they proved the applicability of Voronoï based PTV techniques for particle shapes other than spherical.

Another application has been proposed by Chou and Lee (2009), who analyzed the drying of particles in rotating drums. The occurring flow regimes have been captured via high-speed imaging. Post-processing was performed by applying the PTV-Voronoï algorithm, which was adopted from Capart et al. (2002). As a result Chou and Lee (2009) propose a unique dimensionless flow parameter, which accounts for the combined effects of gravity, particle velocity, particle size and filling level.

Aleixo et al. (2011) applied the PTV-Voronoï technique together with coated seeding particles to investigate velocity profiles in a dam-break situation. Though the contribution does not describe a granular flow, it is an example for further potential of the methodology for other applications.

Generally, the method is limited to small fields of view. To capture larger regions of interest and simultaneously resolve the particles, Spinewine and Zech (2001) described the use of two synchronized cameras. The authors reported results for granular hopper flow based on PTV-Voronoï method, emphasizing the importance of a precise image stitching for accurate flow field representation.

Nevertheless, meaningful information can also be obtained when dividing the region of interest into smaller sub-domains and evaluating them individually, as done in this study. Four fields of view have been used to resolve the total width of the process chamber. The trajectories and associated properties can be described statistically. Moreover, averaged flow fields can be derived and are then available for comparison with the results of the other measurement techniques.

PTV is not affected by bias errors, in contrast to PIV, which has these errors due to cross-correlation algorithms. Nevertheless, the overall measurement accuracy is limited by limited accuracy of particle detection and errors during the particle assignment step (Cierpka et al., 2013). A more detailed discussion on measurement uncertainty of PTV and PIV is given by Kähler et al. (2012).

4. Results and comparison

First, we present the PTV results, which deliver many details that are not accessible with the other measurement techniques. Then, we compare instantaneous and temporally averaged velocity results obtained with the different measurement techniques. The PTV yields particle velocities whenever a particle has been detected in one image and was successfully assigned in the following image of an image series. Correspondingly, instantaneous particle velocities are obtained for each of the four fields of view. In total, 5000 images have been acquired, which represents a process time of 5 s, similar to the PIV experiments. The images were used to average the particle velocity values for the sake of comparison with PIV, LDV and FOP.

Instantaneous particle displacements are combined to obtain individual particle trajectories, as visualized exemplarily in Fig. 3, where each trajectory is colored with velocity magnitude. To improve readability, trajectories are displayed only for the first 20 time steps (0.02 s).

The trajectories show the different particle dynamics within a fluidized bed. Generally, higher velocities, up to 1.5 m/s can be found in the center of the bed where the solid volume fraction is often lower than close to the side-wall and rising gas bubbles primarily affect the particle motion. At the same time, particles in the vicinity of the side-wall have lower velocities. However, there is a difference in direction of particle motion near the side-wall, as can be seen from Fig. 3 as well. Particles in the lower right corner are moving parallel to the side-wall with a low velocity, which is caused by the wall friction and high particle number density. However, particles in the upper right corner impinge upon the side-wall with much higher velocity under an angle and are reflected to assemble on the top of the denser particle bed. Hence, particle–wall collisions can be analyzed beside the individual particle velocities.

The particle trajectories are the fundamental information which can be used to derive process relevant parameters, for instance particle circulation or residence times and associated solid mass fluxes. Moreover, inter-particle collisions are a relevant process parameter which determines, for example, agglomeration efficiency or breakage probability in granulation processes. Particle–particle collisions can be estimated as well, but there are some restrictions. In dilute regions, inter-particle collisions result in discontinuous trajectories which can be evaluated in similar manner as particle–wall collisions. However, these collisions occur seldom and insignificantly contribute to the overall number of collisions. In contrast, particle motion in the dense bed region is dominated by particle–particle collisions. These collision events result in less pronounced particle deflections since there is little free space between the particles. Hence the collision cannot be detected as strong discontinuity of a trajectory. Therefore, it can be analyzed up to now only in qualitative manner or on the basis of collision models (You et al., 2004). Generally, the particle velocity fluctuations are a measure for the particle–particle collisions and are usually described according to the kinetic theory of granular

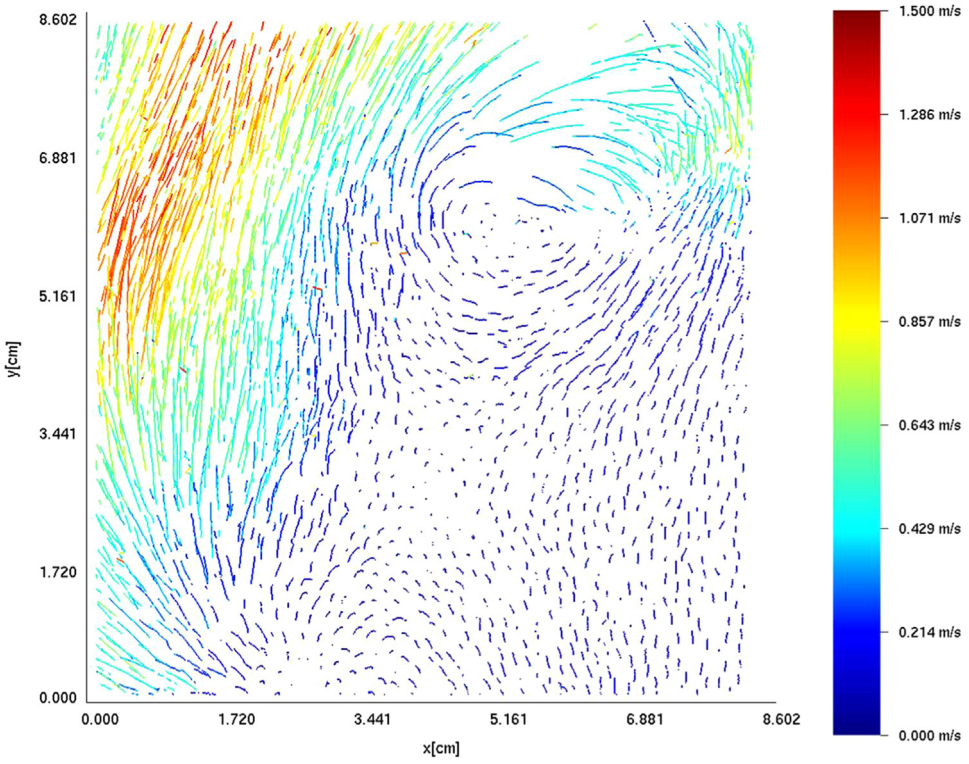

Fig. 3. Particle trajectories over the first 20 time steps, colored with local particle velocity magnitude at a fluidization velocity of $u = 3u_{mf}$ for the field of view located at right side-wall (global x-coordinate from 220 mm to 300 mm). (For interpretation of the references to color in this figure caption, the reader is referred to the web version of this paper.)

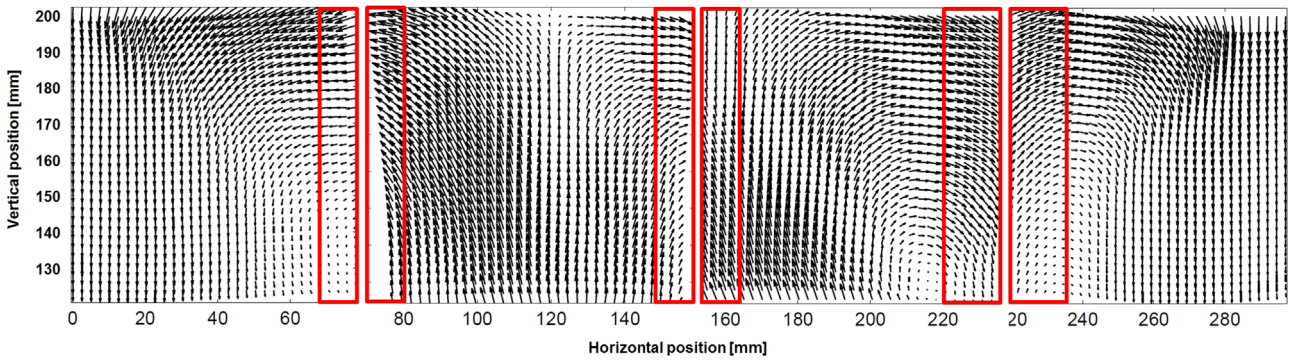

Fig. 4. Temporally averaged Eulerian velocity fields based on PTV results at a fluidization velocity of $u = 3u_{mf}$. Overlapping regions are highlighted using red boxes. (For interpretation of the references to color in this figure caption, the reader is referred to the web version of this paper.)

flow (KTGF) in terms of granular temperature. This property can be obtained for sub-regions in the fields of view, where velocities of a few particles are analyzed with respect to their velocity deviations. Detailed results concerning particle collisions are beyond the scope of this study, which is primarily concerned with particle velocity measurement. However, it is worth mentioning that these details are omitted when using one of the other measurement techniques.

Coming back to the instantaneous particle velocities, they can be used to derive solid phase velocity fields similar to results provided by time-resolved PIV. Interrogating the particle velocities for sub-regions (128 × 128 pixel with an overlap of 75%), locally averaged solid phase velocities can be obtained. A representative Eulerian solid phase velocity field can be derived by temporally averaging instantaneous results, as shown in Fig. 4. The four fields of view are shown from left to right, while overlapping regions are highlighted. This procedure provides complete velocity fields but at the expense of loss in information due to averaging. Mean velocities are assigned to regions where almost no particle could be found, for instance in the bulk region of a rising bubble. This also explains the deviation found within the overlapping areas. The sequential measurement of particle dynamics in the four FOVs is another reason for the deviation.

However, integral process parameters like solid mass fluxes or circulation times can be evaluated from these velocity fields, and this may be even faster than evaluating single particle trajectories, as discussed in the following.

Standard PIV measurements using 10 Hz imaging rate yield instantaneous solid phase velocity fields for the front view of the process chamber. However, this imaging rate is too low for the investigated fluidization pattern to carry out time series analysis. Temporal averaging is used instead to quantify particle circulation motion (Börner, 2013), as shown in Fig. 5.

Fig. 5 shows exemplarily the solid phase velocity field obtained by averaging results from 50 double frames corresponding to 5 s. Instantaneous patterns completely vanish using this kind of visualization. Two counter-rotating vortices can be observed in the lower half of the image. They represent the global particle circulation within the chamber and partially could be observed in the PTV results as well.

However, the velocity vectors, in particular in the upper half of the image, yield the impression of particles falling downwards over the whole cross section of the chamber. This peculiarity of the PIV results is due to the inhomogeneous particle distribution. Standard PIV requires a homogenous seeding and a constant amount of tracer in each interrogation area.

At the same time, FOP measurements are only possible at predefined locations, where the probe can enter the apparatus. Consequently, such measurements yield velocity information

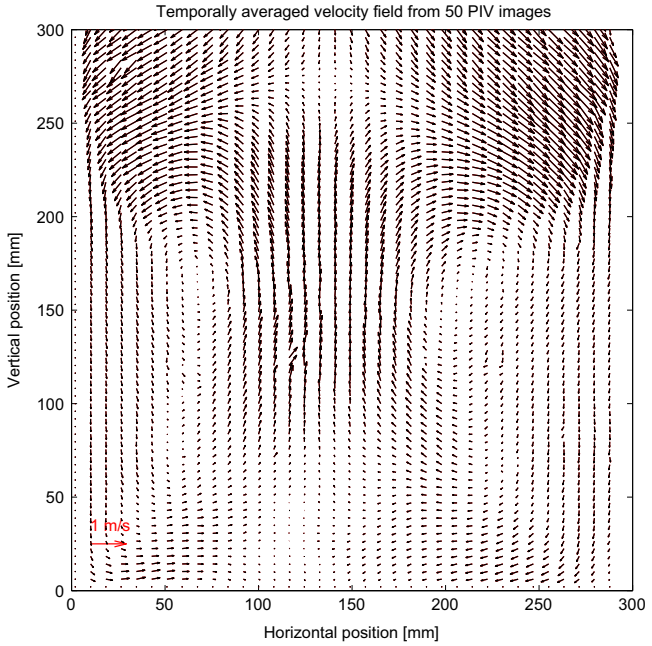

Fig. 5. Averaged velocity field from PIV measurements at a fluidization velocity of $u = 3u_{mf}$. The vector plot is limited to a size of 300 × 300 mm and shows only every second value for an improved readability. A reference vector (1 m/s) is shown in red in the lower left corner. (For interpretation of the references to color in this figure caption, the reader is referred to the web version of this paper.)

(vertical component) only for a few measurement points. Moreover, the mounting of the probes and system initialization are very time consuming. Therefore, since the vertical direction corresponds to the main flow direction, FOP measurements have been realized to obtain this velocity component only. Signals have been acquired for 180 s using a sampling rate of 1000 Hz. Subsequent post-processing occurred in terms of cross-correlating signals from two fiber pairs.

Identical measurement points have been used to estimate the particle velocity on-line with the LDV. Sequentially, the vertical and horizontal velocity components have been measured, which can then be combined to derive representative velocity vectors. A fixed measurement time of $t = 300$ s was specified to acquire a sufficient number of samples. According to Pandey et al. (2004) and Yanta and Smith (1973), 1000 samples are enough to ensure statistically meaningful results. This condition has been fulfilled for the discussed results.

Finally, the time averaged velocity results for FOP, LDV, PIV and PTV can be compared and show remarkable differences at certain

points. Fig. 6 shows velocity profiles for the horizontal and vertical velocity component at a location of $y=200$ mm above the bottom of the chamber.

Both profiles, focusing on the solid line for PIV, correspond to the typical flow pattern of two counter-rotating vortices, as visualized by the global PIV results in Fig. 5.

As aforementioned, the horizontal velocity component has been evaluated only by LDV, PIV and PTV. For PTV, the four different fields of view are plotted with individual symbols so that one can follow their course individually. Generally, the results obtained with the different techniques show a good agreement. Highest deviation occurs between LDV and the two imaging techniques near the side-walls. Here, LDV yields velocities which are almost twice as low (left side-wall) or high (right side-wall) as the PTV and PIV measurements. In the center region, the measurement results collapse onto a single curve, including the same location for the transition from negative to positive horizontal velocity values. The horizontal velocity from PIV and PTV measurements are nearly the same along the complete profile.

The vertical velocity component is shown in the bottom plot of Fig. 6. Here, all four measurement techniques are compared to each other. All measurement techniques show a maximum vertical velocity slightly shifted to the left of the center, between $x=100$ and 150 mm. Similar to the horizontal velocity component, LDV measures the highest/lowest vertical velocities of all devices. However, the trend is identical to that found for the FOP and PIV, which agree fairly well. A larger deviation can be observed for PTV results this time, which show vertical velocities close to zero in the center region around $x=150$ mm.

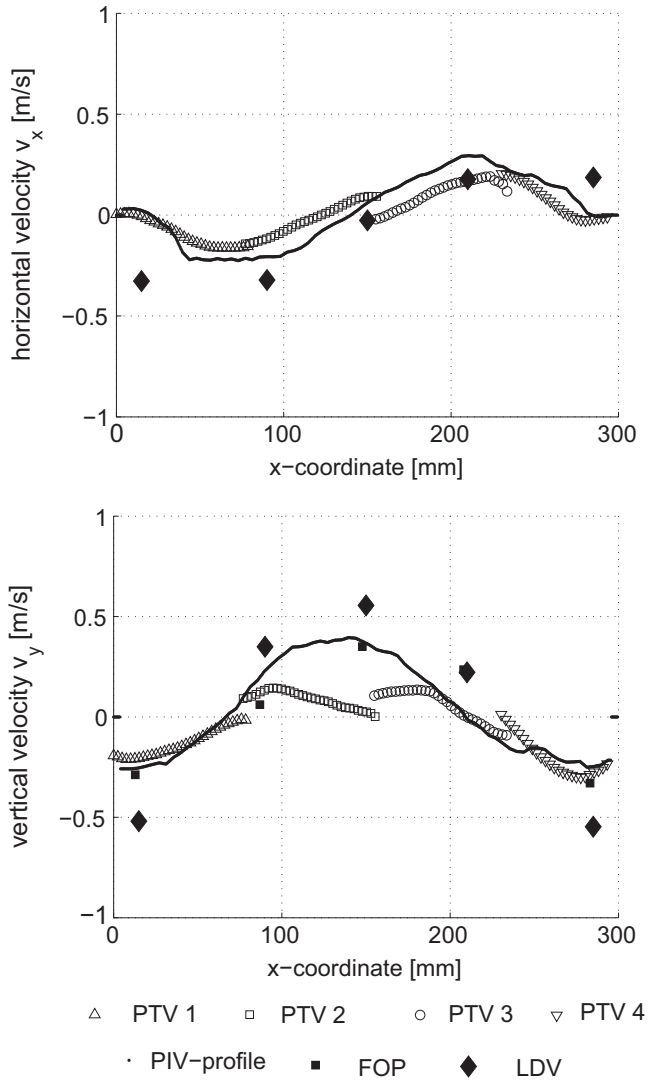

Fig. 6. Comparison of averaged particle phase velocities (horizontal velocity component as upper and vertical velocity component as lower plot) at a vertical position of $y=200$ mm at $3u_{mf}$ for FOP (filled square), LDV (filled diamond), PIV (solid line) and PTV (empty symbols).

An explanation for the differences in the results can be found in the vector plots for PTV (Fig. 4) and PIV (Fig. 5). Comparing the recirculation of the particles, the stagnation point (zero vertical velocity) can be found at $y=200$ mm for PTV while it is located at $y=250$ mm for PIV. This means that either the particles were fluidized at different conditions or PTV and PIV yield different results due to evaluation methodology. Fluidization conditions were controlled using a high precision mass flow controller. This guaranties identical fluidization conditions for all experiments.

A significant difference is present in the averaging procedure of PIV and PTV. PIV uses interrogation areas of 16×16 pixel corresponding to a window side length of approximately 8 mm. A similar interrogation area with a window side length of 10 mm was used for the approximation of a continuous flow field from the PTV data. However, the number of particles in each interrogation area for PTV is not constant. Therefore, a larger number of samples is required to ensure reasonable statistics which is achieved using a higher frame rate of 1000 frames per second for the same measurement time as in PIV (5 s).

5. Recommendations and conclusions

Four measurement techniques, namely fiber optical probe (FOP), laser-Doppler velocimetry (LDV), particle image velocimetry (PIV) and particle tracking velocimetry (PTV) have been applied to a flat fluidized bed apparatus to acquire particle velocity data.

Time resolved results, instantaneous particle velocities and particle trajectories have been presented for an innovative PTV approach and the potential for highly sophisticated analysis of granular flows including the estimation of particle collisions has been discussed.

Furthermore, temporally averaged particle velocity results have been presented for all four measurement techniques. The comparison of these results showed a fair agreement for the vertical velocity component obtained by FOP, LDV and PIV.

In contrast, major deviations have been observed when comparing to results from the PTV method. The sequential nature underlying the PTV measurements is visible throughout the profiles for the vertical velocity component, which partially do not really match. Longer measurement times may improve the averaged results. As a consequence of the high frame rate and limited memory, the PTV method shows a deficit when global solid motion patters are targeted. The measurement time is the most significant difference between the four techniques. While FOP and LDV have been used for 180 and 300 s, respectively, the PIV and PTV measurement times were significantly lower. These measurements took only 5 s.

Finally, recommendation can be given on the accuracy and reliability of the different measurement techniques together with a practical guide for the usage of measurement techniques in dense particle systems. The upper part of Table 4 is used to provide an overview of technical properties which are most decisive for the application of the four techniques. PIV and PTV can be used with almost identical spatial and temporal resolution, while the FOP and LDV provide even higher temporal resolution for local velocity measurements. The spatial resolution of FOP strongly depends on the size of the probe head and the fibers used within the probe. The spatial resolution of LDV depends on the measuring

Table 4
Comparison of advantages and disadvantages for the application of the different measurement techniques to fluidized beds.

Property	FOP	LDV	PIV	PTV
Spatial resolution, field of view	Low resolution, point-wise measurement	Depending on optical parameters and measuring volume, point-wise measurement	High resolution possible, large field of view possible	High resolution required for particle segmentation, therefore restricted field of view
Temporal resolution	Very high	Very high	Low, commonly 10–15 Hz double-frame rate	High resolution, 1000 frames per second at full chip resolution
Velocity measurement range	No limitation	No limitation	0 m/s to supersonic, related to frame rate	0 m/s to supersonic, related to frame rate
Velocity data	Single velocity components	Single velocity components, simultaneous measurement possible, signal coherence reduces sampling rate	Instantaneous solid phase velocity field	Time resolved particle velocities (2D)
Application restrictions	Not restricted, but intrusive	Optical access needed	Optical access needed, data from visible particles	Optical access needed, data from visible particles
Performance for	*Application to fluidized beds*			
High particle concentration	Limiting measuring volume (penetration depth)	Particle occlusion leads to limited sampling rate (penetration depth)	Limiting to 2D PIV	limiting to 2D PTV, first layer particles
Low particle concentration	Low sampling rate	Low sampling rate, but higher penetration depth	Planar PIV yields velocities from particles residing at various depth levels	Planar PTV yields valocities only from first layer particles
Particle size	Adaption by changing probe head, probe head determines maximum particle diameter	Particle sizes larger than detection volume require adapted system settings and validation of results	Not discriminable, insignificant effect on velocity estimation	Minimum particle size determined by spatial resolution and segmentation algorithm
Number of particles in detection zone	Only one particle allowed	Only one particle allowed	No restriction for number, but for resolution, at least 3 pixel per particle diameter	No restriction of number, but of resolution, more particles corresponds to longer computing time
Output data	Voltage signal evaluated by cross-correlation algorithm	Particle velocity component (on-line)	Averaged 2D velocity field based on cross-correlation (this study: 16×16 pixel at 50 % overlap correspond to approximately 64 particles)	Several processing steps yield instantaneous particle velocities, time series delivers Lagrangian trajectories, approximation of 2D velocity field, particle–particle collision
Affection of process	Intrusiveness causes deviating particle velocities	Non-intrusive	Non-intrusive	Non-intrusive
Signal disturbance	Signals from particles and gas bubbles not distinguishable, contamination of probe head	Several particles within the detectionvolume cause wrong velocity values, but almost excluded by large particles in use	window contamination due to particle erosion	Window contamination, assumption of spherical particles violated by fractal material
Calibration procedure and parameters	Calibration of particle velocity and solid volume fraction	No calibration needed, but verification of results from reflection signals required	Spatial calibration to correct image distortion	spatial calibration as for PIV, thresholds in segmentation and Voronoï algorithm

volume size and on the step size of the measurement grid. However, LDV application to large particles (particle diameter comparable to size of measurement volume) is always challenging and requires laborious verification of velocity results. Additionally, LDV is limited to systems which yield optical access. Moreover, the data acquisition is time consuming and prevents from fast velocity estimation.

Even more effort is needed when using the FOP, which requires calibration for each velocity component. The intrusiveness of the FOP compensates for the required optical access to the system, but the influence on the particle systems is an unknown quantity.

The application of image based techniques is more straight forward. PIV and PTV show only one main restriction; they are applicable only to visible particles or quasi-2D configurations. PIV showed some advantages for the investigation of global process pattern and long measurement times, while PTV may provide details from the micro-level based on discrete particle evaluation. The limitations of PTV are linked to hardware limitations like chip size and memory size, which will be overcome with technical development in the future. Although PIV systems will benefit from technical developments as well, the discrete nature of PTV data evaluation is what puts PTV ahead of PIV.

Economically, the FOP is by far the best choice since it can be built with low cost components, while LDV, PIV and PTV require expensive equipment. Moreover, the FOP is the only technique that can be used in pilot or real scale plants. It delivers velocity data which are related to the particle motion, but the estimated velocity is strongly influenced by the gas flow (rising bubbles) and an extensive calibration procedure is required, which are disadvantages when using the FOP. Generally, the estimated particle velocity is lower than in reality, decreasing the reliability of the measurement technique. Eventually, the FOP is the best choice for monitoring and process control in real scale plants.

In research with priority to high precision data, there are many advantages in using image based techniques which are discussed in Table 4. This table provides a comparison of performance parameters of the different techniques relevant for the application to fluidized beds.

The LDV is a technique that works without calibration and has been successfully applied to dense particulate systems. However, an appropriate system setup has to be ensured for the evaluation of scattered light coming from particles which are larger than the measuring volume. The application is limited to systems that provide optical access or when using endoscopic LDV devices. The latter configuration is once again associated with intrusion and disturbance of the particle system and the pointwise measurement is very time consuming.

The PIV is a fast measurement technique to obtain 2D solid phase velocity fields for lab scale apparatuses. Moreover, it is associated with some loss in information when used for global observation of the particle system inside the fluidized bed, as in this study. Comparing the interrogation area size with the typical particle dimension, a representative velocity vector is determined by the cross-correlation algorithm for an area that may comprise up to 16 individual particles. This results in a smoothing of the velocity field, in particular for regions with high velocity gradients which are typical for fluidized beds. Nevertheless, the global motion of the solids can be captured with reasonable accuracy for larger fields of view and longer observation times. Macro-scale parameters like solid mass fluxes or circulation times can be evaluated on this basis. Micro-scale quantities like collision rates are not provided by PIV and can only be estimated using PTV.

The PTV technique shows many features identical to PIV, but at smaller fields of view and shorter observation times. It yields individual particle velocities for a restricted region of the process volume and, therefore can be best used for research purposes. Applying PTV to several fields of view may provide information for larger process chambers. However, the information acquired in this manner can be associated only in case of quasi-stationary processes. Decisive micro-process properties, for instance particle–particle interactions, can be captured by PTV. This is a unique feature of PTV and makes this technique so attractive.

Eventually, the decision whether using PIV or PTV is associated to a compromise. One can either obtain macro-scale process parameters using PIV or acquire highly resolved data for discrete particle analysis with PTV. The developments of imaging hardware and computer technique will improve capabilities of PTV. Consequently, it will be an important tool in future particle technology research and development processes.

Acknowledgments

The authors gratefully acknowledge the funding of this work by the German Federal Ministry of Science and Education (BMBF) as part of the InnoProfile-Transfer project NaWiTec (03IPT701X). Moreover, we thank Christian Knopf for supporting the experiments and the colleagues from the Laboratory of Fluid Dynamics and Technical Flows of the Otto von Guericke University Magdeburg, in particular Christoph Roloff, for helpful discussions and technical support.

References

Adrian, R., 1991. Particle-imaging techniques for experimental fluid mechanics. Annu. Rev. Fluid. Mech. 23 (1), 261–304.
Agarwal, G., Lattimer, B., Ekkad, S., Vandsburger, U., 2012. Experimental study on solid circulation in a multiple jet fluidized bed. AIChE J. 58, 3003–3015.
Ahn, H., Brennen, C., Sabersky, R., 1991. Measurements of velocity, velocity fluctuation, density, and stresses in chute flows of granular materials. Trans. ASME J. Appl. Mech. 58 (3), 792–803.
Albrecht, H.-E., Borys, M., Damaschke, N., Tropea, C., 2003. Laser Doppler and Phase Doppler Measurement Techniques. Springer.
Aleixo, R., Soares-Frazão, S., Zech, Y., 2011. Velocity-field measurements in a dam-break flow using a PTV Voronoï imaging technique. Exp. Fluids 50 (6), 1633–1649.
Beaud, F., Louge, M., 1996. Similarity of radial profiles of solid volume fraction and in a circulating fluidised bed. In: Large, J., Laguérie, C. (Eds.), Fluidization VIII. Engineering Foundation, pp. 97–104.
Bendicks, C., Tarlet, D., Roloff, C., Bordás, R., Wunderlich, B., Michaelis, B., Thévenin, D., 2011. Improved 3-D particle tracking velocimetry with colored particles. J. Signal Inf. Proc. 2 (2), 59–71.
Bhusarapu, S., Al-Dahhan, M., Duduković, M., 2006. Solids flow mapping in a gas-solid riser: mean holdup and velocity fields. Powder Technol. 163 (1), 98–123.
Boateng, A., Barr, P., 1997. Granular flow behaviour in the transverse plane of a partially filled rotating cylinder. J. Fluid Mech. 330, 233–249.
Bokkers, G.A., van SintAnnaland, M., Kuipers, J.A.M., 2004. Mixing and segregation in a bidisperse gas–solid fluidised bed: a numerical and experimental study. Powder Technol. 140, 176–186.
Börner, M., 2013. Feststoffdynamik und Partikelverweilzeit am Beispiel der Top-Spray Wirbelschichtsprühgranulation (Dissertation). University of Magdeburg.
Börner, M., Hagemeier, T., Ganzer, G., Peglow, M., Tsotsas, E., 2014. Experimental spray zone characterization in top-spray fluidized bed granulation. Chem. Eng. Sci. 116, 317–330.
Börner, M., Peglow, M., Tsotsas, E., 2011. Particle residence times in fluidized bed granulation equipments. Chem. Eng. Technol. 34 (7), 1116–1122.
Börner, M., Peglow, M., Tsotsas, E., 2013. Derivation of parameters for a two compartment population balance model of Wurster fluidised bed granulation. Powder Technol. 238, 122–131.
Breault, R., Guenther, C., Shadle, L., 2008. Velocity fluctuation interpretation in the near wall region of a dense riser. Powder Technol. 182, 137–145.
Breault, R., Ludlow, C., Yue, P., 2005. Cluster particle number and granular temperature for cork particles at the wall in the riser of a cfb. Powder Technol. 149, 68–77.
Capart, H., Young, D.L., Zech, Y., 2002. Voronoï imaging methods for the measurement of granular flows. Exp. Fluids 32 (1), 121–135.
Chemloul, N., Benrabah, O., 2008. Measurement of velocities in two-phase flow by laser velocimetry: interaction between solid particles motion and turbulence. J. Fluids Eng. 130, 071301.
Chou, H.-T., Lee, C.-F., 2009. Cross-sectional and axial flow characteristics of dry granular material in rotating drums. Granul. Matter 11 (1), 13–32.
Cierpka, C., Lütke, B., Kähler, C.J., 2013. Higher order multi-frame particle tracking velocimetry. Exp. Fluids 54 (5), 1–12.

Cloete, S., Zaabout, A., Johansen, S., Annaland, v.Sint, Gallucci, M., Amini, S., 2013. The generality of standard 2D TFM approach in predicting bubbling fluidized bed hydrodynamics. Powder Technol. 235, 735–746.

Cocco, R., Cleveland, J., Harner, R., Chrisman, R., 1995. Simultaneous in-situ determination of particle loadings and velocities in a gaseous medium. AIChE Symp. Ser. 91 (308), 147–153.

Cronin, K., Çatak, M., Tellez-Medina, D., Cregan, V., O'Brien, S., 2010. Modelling of particle motion in an internal re-circulatory fluidized bed: pharmaceutical granulation and processing. Chem. Eng. J. 164 (2–3), 393–402.

de Jong, J., Odu, S., v. Buijtenen, M., Deen, N., v. Sint Annaland, M., Kuipers, J., 2012. Development and validation of a novel digital image analysis method for fluidized bed particle image velocimetry. Powder Technol. 230, 193–202.

de Jong, J., v. Sint Annaland, M., Kuipers, J., 2013. Experimental study on the hydrodynamic effects of gas permeation through horizontal membrane tubes in fluidized beds. Powder Technol. 241, 74–84.

Dencs, B., 1995. Particle velocity measurements in dense fluidized beds. Part. Part. Syst. Charact. 12 (6), 314–317.

Depypere, F., Pieters, J., Dewettinck, K., 2009. Pept visualisation of particle motion in a tapered fluidised bed coater. J. Food Eng. 93, 324–336.

Durst, F., Melling, A., Whitelaw, J., 1976. Principles and Practice of Laser-Doppler Anemometry. NASA STI/Recon Technical Report A 76, 47019.

Durst, F., Melling, A., Whitelaw, J., 1981. Principles and Practice of Laser-Doppler Anemometry, Vol.2. Academic Press, London.

Hagemeier, T., Roloff, C., Bück, A., Tsotsas, E., Estimation of particle dynamics in 2-d fluidized beds using particle tracking velocimetry. Particuology, http://dx.doi.org/10.1016/j.partic.2014.08.004, in press.

Hartge, E.-U., Werther, J., 1988. Solids concentration and velocity patterns in circulating fluidized beds. In: Basu, P., Large, J. (Eds.), Circulating Fluidized Bed Technology II. Pergamon Press, pp. 165–180.

Herbert, P., Gauthier, T., Briens, C., Bergougnou, M., 1994. Application of fiber optic reflection probes to the measurement of local particle velocity and concentration in gas–solid flow. Powder Technol. 80 (3), 243–252.

Hernández-Jiménez, F., Sánchez-Delgado, S., Gómez-García, A., Acosta-Iborra, A., 2011. Comparison between two-fluid model simulations and particle image analysis& velocimetry (PIV) results for a two-dimensional gas-solid fluidized bed. Chem. Eng. Sci. 66, 3753–3772.

Hoomans, B.P.B., Kuipers, J.A.M., MohdSalleh, M.A., Stein, M., Seville, J.P.K., 2001. Experimental validation of granular dynamics simulations of gas-fluidised beds with homogenous in-flow conditions using positron emission particle tracking. Powder Technol. 116 (2–3), 166–177.

Horio, M., Kobylecki, R., Tsukada, M., 2003. Measurements and instrumentation. In: Yang (Ed.), Handbook of Fluidization and Fluid–Particle Systems. Marcel Dekker, New York, pp. 643–704.

Hsiau, S., Hunt, M., 1993. Shear-induced particle diffusion and longitudinal velocity fluctuations in a granular-flow mixing layer. J. Fluid Mech. 251, 299–313.

Hsiau, S.-S., Jang, H.-W., 1998. Measurements of velocity fluctuations of granular materials in a shear cell. Exp. Therm. Fluid Sci. 17 (3), 202–209.

Hussain, M., Kumar, J., Peglow, M., Tsotsas, E., 2014. On two-compartment population balance modeling of spray fluidized bed agglomeration. Comput. Chem. Eng. 61, 185–202.

Ibsen, C., Solberg, T., Hjertager, B., Johnsson, F., 2002. Laser Doppler anemometry measurements in a circulating fluidized bed of metal particles. Exp. Therm. Fluid Sci. 26, 851–859.

Ishida, M., Shirai, T., Nishiwaki, A., 1980. Measurement of the velocity and direction of flow of solid particles in a fluidized bed. Powder Technol. 27 (1), 1–6.

Jesuthasan, N., Baliga, B., Savage, S., 2006. Use of particle tracking velocimetry for measurements of granular flows: review and application-particle tracking velocimetry for granular flow measurements. Kona 24, 15.

Johnsson, H., Johnsson, F., 2001. Measurements of local solids volume-fraction in fluidized bed boilers. Powder Technol. 115 (1), 13–26.

José, M.S., Alvarez, S., Morales, A., Olazar, M., Bilbao, J., 2006. Solid cross-flow into the spout and particle trajectories in conical spouted beds consisting of solids of different density and shape. Chem. Eng. Res. Des. 84 (6), 487–494.

Kähler, C.J., Scharnowski, S., Cierpka, C., 2012. On the uncertainty of digital PIV and PTV near walls. Exp. Fluids 52 (6), 1641–1656.

Keane, R., Adrian, R., 1991. Optimization of particle image velocimeters: II. Multiple pulsed systems. Meas. Sci. Technol. 2 (10), 963–974.

Kellay, H., Amarouchene, Y., Boudet, J., 2007. Intermittency of the velocity fluctuations in a granular surface flow. Phys. Fluids 19, 078104.

Laverman, J., Roghair, I., v. Sint Annaland, M., Kuipers, H., 2008. Investigation into the hydrodynamics of gas–solid fluidized beds using particle image velocimetry coupled with digital image analysis. Can. J. Chem. Eng. 86, 523–535.

Laverman, J., Roghair, I., v. Sint Annaland, M., Kuipers, J., 2007. Experimental study on solids mixing and bubble behavior in a pseudo-2D freely bubbling, gas–solid fluidized bed using PIV and DIA. In: Proceedings of Sixth International Conference on Multiphase Flow, Leipzig, Germany.

Li, S., Yang, H., Zhang, H., Yang, S., Lu, J., Yue, G., 2009. Measurements of solid concentration and particle velocity distributions near the wall of a cyclone. Chem. Eng. J. 150 (1), 168–173.

Lim, E., Wong, Y., Wang, C.-H., 2007. Particle image velocimetry experiment and discrete-element simulation of voidage wave instability in a vibrated liquid-fluidized bed. Ind. Eng. Chem. Res. 46 (4), 1375–1389.

Lim, K., Agarwal, P., 1992. Bubble velocity in fluidized beds: the effect of non-vertical bubble rise on its measurement using submersible probes and its relationship with bubble size. Powder Technol. 69, 239–248.

Link, J., Godlieb, W., Tripp, P., Deen, N., Heinrich, S., Kuipers, J., Schönherr, M., Peglow, M., 2009. Comparison of fibre optical measurements and discrete element simulations for the study of granulation in a spout fluidized bed. Powder Technol. 189 (2), 202–217.

Link, J., Zeilstra, C., Deen, N., Kuipers, H., 2004. Validation of a discrete particle model in a 2D spout-fluid bed using non-instrusive optical measuring techniques. Can. J. Chem. Eng. 82, 30–36.

Liu, G.-Q., Li, S.-Q., Zhao, X.-L., Yao, Q., 2008. Experimental studies of particle flow dynamics in a two-dimensional spouted bed. Chem. Eng. Sci. 63 (4), 1131–1141.

Louge, M., 1997. Experimental techniques. In: Grace, J., Avidan, A. (Eds.), Circulating Fluidized Beds. Blackie Academic & Professional, pp. 312–368.

Luchnikov, V., Medvedev, N., Oger, L., Troadec, J.-P., 1999. Voronoi-Delaunay analysis of voids in systems of nonspherical particles. Phys. Rev. E 59 (6), 7205–7212.

Mohs, G., Gryczka, O., Heinrich, S., Mörl, L., 2009. Magnetic monitoring of a single particle in a prismatic spouted bed. Chem. Eng. Sci. 64 (23), 4811–4825.

Mychkovsky, A., Rangarajan, D., Ceccio, S., 2012. Ldv measurements and analysis of gas and particulate phase velocity profiles in a vertical jet plume in a 2D bubbling fluidized bed part 1: a two-phase LDV measurement technique. Powder Technol. 220, 55–62.

Natarajan, V., Hunt, M., Taylor, E., 1995. Local measurements of velocity fluctuations and diffusion coefficients for a granular material flow. J. Fluid Mech. 304, 1–25.

Olazar, M., 1998. Measurement of particle velocities in conical spouted beds using an optical fiber probe. Ind. Eng. Chem. Res. 37 (11), 4520–4527.

Pandey, P., Turton, R., Yue, P., Shadle, L., 2004. Nonintrusive particle motion studies in the near-wall region of a pilot-scale circulating fluidized bed. Ind. Eng. Chem. Res. 43, 5582–5592.

Patrose, B., Caram, H., 1982. Optical fiber probe transit anemometer for particle velocity measurements in fluidized beds. AIChE J. 28 (4), 604–609.

Raffel, M., Willert, C., Wereley, S., Kompenhans, J., 2007. Particle Image Velocimetry: A practical guide. Springer.

Rensner, D., 1991. Faseroptische sensoren für feststoffbeladene strömungen.

Rensner, D., Werther, J., 1993. Estimation of the effective measuring volume of single-fibre reflection probes for solid volume concentration measurements. Part. Part. Syst. Charact. 10 (2), 48–55.

Rix, S., Glass, D., Greated, C., 1996. Preliminary studies of elutriation from gas-fluidised beds using particle image velocimetry. Chem. Eng. Sci. 51 (13), 3479–3489.

San José, M., Olazar, M., Alvarez, S., Izquierdo, M., Bilbao, J., 1998. Solid cross-flow into the spout and particle trajectories in conical spouted beds. Chem. Eng. Sci. 53 (20), 3561–3570.

Sánchez-Delgado, S., Marugán-Cruz, C., Acosta-Iborra, A., Santana, D., 2010. Dense-phase velocity fluctuation in a 2-D fluidized bed. Powder Technol. 200, 37–45.

Sánchez-Delgado, S., Marugán-Cruz, C., Soria-Verdugo, A., Santana, D., 2013. Estimation and experimental validation of the circulation time in a 2D gas–solid fluidized beds. Powder Technol. 235, 669–676.

Santana, D., Nauri, S., Acosta, A., García, N., Macías-Machín, A., 2005. Initial particle velocity spatial distribution from 2-D erupting bubbles in fluidized beds. Powder Technol. 150, 1–8.

Savage, S., 1979. Gravity flow of cohesionless granular materials in chutes and channels. J. Fluid Mech. 92 (1), 53–96.

Spinewine, B., Capart, H., Larcher, M., Zech, Y., 2003. Three-dimensional Voronoï imaging methods for the measurement of near-wall particulate flows. Exp. Fluids 34 (2), 227–241.

Spinewine, B., Zech, Y., 2001. Digital imaging characterisation of a granular hopper flow. In: Proceedings of Partec-International Congress for Particle Technology, Nürnberg, Germany. pp. 1–8.

Stanislas, M., Okamoto, K., Kähler, C., Westerweel, J., 2005. Main results oft he second international PIV challenge. Exp. Fluids 39, 170–191.

Sutkar, V., Deen, N., Kuipers, J., 2013. Spout fluidized beds: recent advances in experimental and numerical studies. Chem. Eng. Sci. 86, 124–136.

Tayebi, D., Svendsen, H., Grislingas, A., Mejdell, T., Johannessen, K., 1999. Dynamics of fluidized-bed reactors. Development and application of a new multi-fiber optical probe. Chem. Eng. Sci. 54 (13-14), 2113–2122.

Tropea, C., Yarin, A., Foss, J., 2007. Handbook of Experimental Fluid Mechanics. Springer.

Tsuji, Y., Morikawa, Y., 1982. LDV measurements of an air–solid two-phase flow in a horizontal pipe. J. Fluid Mech. 120 (1), 385–409.

Tsuji, Y., Morikawa, Y., Shiomi, H., 1984. LDV measurements of an air–solid two-phase flow in a vertical pipe. J. Fluid Mech. 139, 417–434.

v. Buijtenen, M., Börner, M., Deen, N., Heinrich, S., Antonyuk, S., Kuipers, J., 2011a. An experimental study of the effect of collision properties on spout fluidized bed dynamics. Powder Technol. 206, 139–148.

v. Buijtenen, M., v. Dijk, W.-J, Deen, N., Kuipers, J., Leadbeater, T., Parker, D., 2011. Numerical and experimental study on multiple-spout fluidized beds. Chem. Eng. Sci. 66, 2368–2376.

Wang, Z., Bi, H., Lim, C., 2009. Measurements of local flow structures of conical spouted beds by optical fibre probes. Can. J. Chem. Eng. 87 (2), 264–273.

Werther, J., 1999. Measurement techniques in fluidized beds. Powder Technol. 102 (1), 15–36.

Westerweel, J., 1997. Fundamentals of digital particle image velocimetry. Meas. Sci. Technol. 8 (12), 1379–1392.

Wu, C., Berrouk, A., 2009. Comments on: solid cross-flow into the spout and particle trajectories in conical spouted beds, by San Josée, Maria J. et al., Chem. Eng. Sci. 53 (1998) 3561–3570. Chem. Eng. Sci. 64(21), 4457–4459.

Xu, J., Zhu, J., 2012. A new method for the determination of cluster velocity and size in a circulation fluidized bed. Ind. Eng. Chem. Res. 51, 2143–2151.

Xu, J., Zhu, J.-X., 2010. Experimental study on solids concentration distribution in a two-dimensional circulating fluidized bed. Chem. Eng. Sci. 65 (20), 5447–5454.
Yanta, W., Smith, R., 1973. Measurements of turbulence-transport properties with a laser Doppler velocimeter. In: American Institute of Aeronautics and Astronautics, Aerospace Sciences Meeting, 11th, Washington, DC.
You, C., Zhao, H., Cai, Y., Qi, H., Xu, X., 2004. Experimental investigation of interparticle collision rate in particulate flow. Int. J. Multiphase Flow 30, 1121–1138.
Zhang, H., Johnston, P., Zhu, J.-X., deLasa, H., Bergougnou, M., 1998. A novel calibration procedure for a fiber optic solids concentration probe. Powder Technol. 100 (2–3), 260–272.
Zhao, X.-L., Li, S.-Q., Liu, G.-Q., Song, Q., Yao, Q., 2008. Flow patterns of solids in a two-dimensional spouted bed with draft plates: PIV measurement and DEM simulations. Powder Technol. 183, 79–87.
Zhou, H., Lu, J., Lin, L., 2000. Turbulence structure of the solid phase in transition region of a circulation fluidized bed. Chem. Eng. Sci. 55, 839–847.
Zhou, J., Grace, J., Lim, C., Brereton, C., 1995. Particle velocity profiles in a circulation fluidized bed riser of square cross-section. Chem. Eng. Sci. 50, 237–244.
Zhu, J.-X., Li, G.-Z., Qin, S.-Z., Li, F.-Y., Zhang, H., Yang, Y.-L., 2001. Direct measurements of particle velocities in gas–solids suspension flow using a novel five-fiber optical probe. Powder Technol. 115 (2), 184–192.